*Journal of Thermal Analysis and Calorimetry, Vol. 75 (2004) 559–567*

# SOLID-STATE CHELATES OF ETHYLENEDIAMINE-TETRAACETATE WITH ALKALI EARTH METALS

*A. B. S. Moitinho, E. Y. Ionashiro, G. R. de Souza and F. L. Fertonani*[*]

Instituto de Química, Universidade Estadual Paulista, Araraquara, São Paulo C.P. 355
CEP 14.800-900, Brazil

## Abstract

Solid-state M-EDTA chelates, where *M* represents the divalent ions Mg(II), Ca(II), Sr(II) or Ba(II) and EDTA is ethylenediaminetetraacetate anion, were synthesized. Thermogravimetry, derivative thermogravimetry (TG, DTG), differential scanning calorimetry (DSC) and X-ray diffraction powder patterns have been used to characterize and to study the thermal behaviour of these chelates. The results provided information concerning the stoichiometry, crystallinity, thermal stability and thermal decomposition.

**Keywords:** alkali earth metals, EDTA, thermal behaviour

## Introduction

Several metal-ion chelates of ethylenediaminetetraacetate (EDTA) anion have been investigated in the solid-state. Moeller *et al.* [1] described the nature of the solid-state chelates of the type H[Ln (EDTA)] and their sodium salt using infrared spectroscopy, DTA, X-ray diffraction and light rotation measurements, in an attempt to characterize these compounds. Sawyer and Paulsen [2] have investigated the properties and infrared spectra of EDTA chelates with several divalent ions. Wendlandt *et al.* [3–5] published more complete studies of the thermal properties of a number of EDTA complexes. Kolat and Powel [6] extended Moeller's work and investigated a series of lanthanide chelates using several techniques, including TG, to study the dehydration of these compounds.

Charles [7] investigated the thermal properties of some solid neodymium complexes derived from ethylenediaminetetraacetic acid by TG and DTA. Bhat and Krishna Iyer [8] described the thermal decomposition of EDTA complexes of Ca(II), Ba(II), Co(II), Cu(II), Ni(II), Bi(II), Sb(III) and Dy(III) ions in solid-state using TG techniques in both air and nitrogen atmosphere. Mercadante *et al.* [9] described the preparation and thermal decomposition of lanthanides(III) and yttrium(III) chelates of ethylenediaminetetraacetic acid and Crespi *et al.* [10] described the preparation and thermal decomposition of Co(II), Ni(II), Cu(II) and Zn(II) chelates of ethylene-

* Author for correspondence: E-mail: fertonan@iq.unesp.br

*1388–6150/2004/ $ 20.00*

*Akadémiai Kiadó, Budapest*
*Kluwer Academic Publishers, Dordrecht*

diaminetetraacetic acid. Rojo *et al.* [11] described the preparation and characterization of the bimetallic chelates of EDTA and DTPA (MM'L·$n$$H_2O$: *L*=EDTA or DTPA and *M*, *M*'=Bi(III), Pb(II), Sr(II), Ca(II) and Cu(II)) by elemental analysis, spectroscopic techniques, X-ray diffraction and thermal analysis (TG and DSC). Insausti *et al.* [12] described the preparation, crystalline structure determination and thermal decompositions of bimetallic chelates, MCuEDTA·$n$$H_2O$, where *M* is Ca(II), Sr(II) and Ba(II) ions as molecular precursors for $MCuO_2$ oxides.

Hoard *et al.* [13] described the preparation and the structural determination of hexaaquomagnesium dihydrogenethylenediaminetetraacetate complex, $[Mg(OH_2)_6H_2EDTA]$. Polynova *et al.* [14, 15] synthesized and determined, by X-ray diffraction analysis, different bimetallic EDTA and HEDTA chelates, of structural formula of $(M'(H_2O)_2[CoHEDTA(H_2O)]_2)_{2\infty}\cdot 2H_2O$, where *M* is Ca(II), Sr(II) and Ba(II) [14] and $\{Sr(H_2O)_3[CoEDTA(H_2O)]\}_{3\infty}\cdot H_2O$ [15]. Sergienko *et al.* [16] synthesized and determined the crystalline structure of the $[Ni(Phen)_3][Ca(EDTA)(H_2O)_2]\cdot 10.5H_2O$.

In this work, solid-state chelates of the alkali earth metals Mg, Ca, Sr and Ba, with EDTA were prepared and investigated by thermoanalytical techniques (TG, DTG, DSC) and X-ray powder diffractometry.

## Experimental

Dihydrogenethylenediaminetetraacetate ($H_2Y^{2-}$) chelates of alkali earth metals, magnesium, calcium, strontium and barium, were obtained by a neutralization reaction, in aqueous media, of the corresponding metal carbonates with a slight excess of $H_4Y$. The partially dissolved mixture was heated in a water bath at 80ºC (to facilitate evolution of $CO_2$) until the gas evolution ceased. After cooling, the solution was filtered using a Whatman nº44 filter paper to separate residual $H_4Y$. These solutions were evaporated to dryness in a water bath and the obtained crystalline solids were kept in a desiccator over anhydrous calcium chloride.

The metallic content of the chelates was directly determined by complexometric titration with a standard $Na_2H_2Y\cdot 2H_2O$ solution, after samples of the compounds had been ignited to either metal oxide or carbonate and dissolved in diluted hydrochloric acid solution; the same metallic content was also determined by TG curves.

The water and ligand contents were determined from TG curves and are in accordance with elemental analysis.

The X-ray powder patterns were obtained with Siemens D-5000 X-ray diffractometer equipment, using $CuK_\alpha$ radiation ($\lambda$=1.541 Å) and settings of 40 kV and 30 μA. The data generated from the XRD were treated using a software AFPAR, Complex des Programme, CNRS, France. This program was utilized to determine the lattice parameters of the synthesized species [17]. This method makes use of the experimental interplanar spacings (*d*-spacing), and data were taken from an original prototype, like $[Mg(OH_2)_6H_2EDTA]$ (values of lattice parameters and the respective reflections) [13], both of which were put together to obtain the experimental lattice parameters [18, 19].

The TG, DTG and DSC curves were obtained with a Mettler TA-4000 thermal analysis system, and an air flow of about 150 mL $min^{-1}$, the temperature ranging from 30 to 900°C to TG curves and 30 to 600°C to DSC curves, a heating rate of 20ºC $min^{-1}$ and samples of about 7 mg. An alumina crucible was used for TG and DTG curves, and an aluminum crucible with a perforated cover for the DSC curves.

## Results and discussion

Table 1 presents the analytical and thermoanalytical (TG) data on the synthesized complexes, from which the general formula $[M(H_2O)_m(H_2Y)]\cdot nH_2O$ can be established, where *M*=Mg, Ca, Sr or Ba, $H_2Y^{2-}$=dihydrogenethylenediaminetetraacetate anion, and $0 \leq m \leq 6$ and $0 \leq n \leq 2$.

**Table 1** Analytical and thermoanalytical results

| Compound | Ligand loss/% | | Metal content/% | | |
|---|---|---|---|---|---|
| | TG | calc. | TG | calc. | EDTA |
| $[Mg(OH_2)_6(H_2Y)]$ | 90.31 | 90.47 | 5.84 | 5.75 | 5.83 |
| $[Ca(OH_2)_2(H_2Y)]$ | 84.78 | 84.68 | 10.87 | 10.94 | 10.89 |
| $[Sr(H_2Y)]\cdot 2H_2O$ | 67.45 | 64.34 | 21.12 | 21.17 | 21.02 |
| $[Ba(OH_2)_6(H_2Y)]\cdot 1.5H_2O$ | 58.31 | 58.23 | 29.33 | 29.06 | 29.10 |

$H_2Y$ – dihydrogenethylenediaminetetraacetate anion ($H_2Y^{2-}$), TG – determined from the TG curves, calc. – calculated value, EDTA – determined by EDTA titration

The X-ray powder patterns, presented in Fig. 1, show that magnesium and calcium complexes have a crystalline structure whereas for the strontium and barium complexes, the diffraction patterns indicate an amorphous state. The X-ray diffraction data obtained to the magnesium complex and those simulated (*d*-spacing and reflections values) from lattice parameter data obtained from the specialized literature [13] are shown in Table 2. Data show that the diffraction lines correspond to $[Mg(OH_2)_6(H_2Y)]$ species as proposed by Hoard *et al.* [13]. From all of the experimental interplanar spacings and the lattice parameters (*a*, *b* and *c* and β angle value) obtained for an original prototype of $[Mg(OH_2)_6(H_2Y)]$ [13], the experimental lattice parameters were generated. The comparison of the lattice parameters generated from experimental data (Table 2), *a*=7.776(4)**, *b*=13.485(6), *c*=8.373(4) Å and β=91.51(4)° with the prototype reported in [13], *a*=7.781(1), *b*=13.478(2), *c*=8.385(1) Å and β=91.55°, suggests that all values are quite similar (*a*=0.06%, *b*=0.05%, *c*=0.1%, β=0.04%).

The calcium complex was not investigated because the experimental *d*-spacing values were not in agreement with the prototype data, available in specialized literature. The crystalline structure of the calcium complex is still being determined.

** Values in parenthesis is the estimated standard deviation.

**Table 2** XRD experimental data obtained for the complex $[Mg(OH_2)_6(H_2Y)]$ identification

| 2θ/degree | *d*-spacing (exp.) | *d*-spacing* | Reflections* |
|---|---|---|---|
| 11.433 | 7.7334 | 7.7781 | 1 0 0 |
| 16.738 | 5.2923 | 5.2520 | 0 2 1 |
| 25.340 | 3.5119 | 3.5106 | 1 3 1 |
| 26.429 | 3.3696 | 3.3695 | 0 4 0 |
| 29.041 | 3.0722 | 3.0653 | 0 3 2 |
| 30.708 | 2.9091 | 2.9112 | 1 4 –1 |
| 31.700 | 2.8203 | 2.8262 | 2 1 –2 |
| 32.680 | 2.7379 | 2.7362 | 0 1 3 |
| 34.657 | 2.5861 | 2.5811 | 0 2 3 |
| 35.239 | 2.5848 | 2.5460 | 3 1 0 |
| 36.735 | 2.4445 | 2.4480 | 2 4 –1 |
| 40.098 | 2.2469 | 2.2463 | 0 6 0 |
| 41.528 | 2.1727 | 2.1750 | 2 2 –3 |
| 45.225 | 2.0034 | 2.0051 | 2 3 3 |
| 46.765 | 1.9409 | 1.9444 | 4 0 0 |
| 46.765 | 1.9409 | 1.9399 | 0 5 3 |
| 49.034 | 1.8563 | 1.8570 | 3 1 3 |
| 50.762 | 1.7971 | 1.7982 | 2 2 –4 |
| 57.256 | 1.6077 | 1.6083 | 3 0 4 |
| 58.179 | 1.5844 | 1.5841 | 1 2 5 |
| 59.320 | 1.5566 | 1.5562 | 4 5 –1 |
| 66.430 | 1.4062 | 1.4060 | 1 5 –5 |
| 69.540 | 1.3507 | 1.3530 | 1 2 –6 |

*Values simulated from lattice parameter data obtained from [13]

The TG and DTG curves of the synthesized complexes are shown in Fig. 2. These curves show basically mass losses in three steps, being: 1 – the first mass loss due to dehydration, except to calcium complex; 2 – removal of the coordinated water molecules simultaneously to ligand pyrolysis and 3 – the formation of inorganic residue (metal oxides or carbonates depending on the thermal stability). The first process for magnesium, strontium and barium complexes can be linked with dehydration, which occurs in only one step, in a general way, but with different kinetic rates (Fig. 2). For the magnesium and calcium complex, water is removed at fairly high temperatures, above 150 and 230ºC (DTG peak) in comparison with strontium and barium crystallization ones (near 70°C). For the calcium complex, water molecules were removed along with the thermal decomposition of the anhydrous complex, indicating that it is strongly coordinated to the metallic center when compared to the mag-

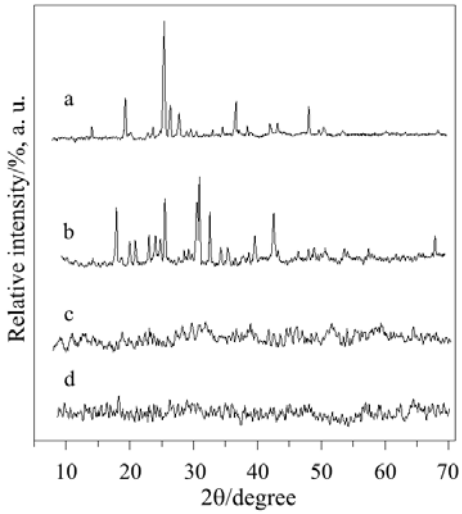


**Fig. 1** X-ray powder diffraction patterns of the complexes: a – $[Mg(OH_2)_6(H_2Y)]$, b – $[Ca(OH_2)_2(H_2Y)]$, c – $[Sr(H_2Y)]\cdot 2H_2O$, d – $[Ba(OH_2)(H_2Y)]\cdot 1.5H_2O$

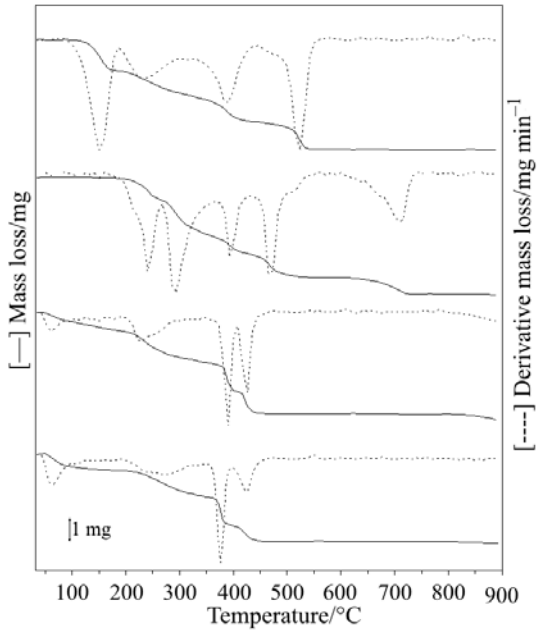


**Fig. 2** TG and DTG curves of the complexes: a – $[Mg(OH_2)_6(H_2Y)]$, b – $[Ca(OH_2)_2(H_2Y)]$, c – $[Sr(H_2Y)]\cdot 2H_2O$, d – $[Ba(OH_2)(H_2Y)]\cdot 1.5H_2O$. $30 \leq \Delta T \leq 900$°C, $\beta$=20°C min$^{-1}$, air flow=150 mL min$^{-1}$, alumina crucible

nesium complex. The same behaviour is observed to the barium complex where the last water is also removed similarly to the calcium complex, that is, above 200ºC. For the magnesium and calcium complexes the results are in agreement with the literature data [13] and [8], respectively; however, for the barium complex the result is in disagreement with [8].

*Magnesium complex*

The TG and DTG curves, Fig. 2a and Table 3 show mass losses in four steps between 90 and 550ºC; the first step up to 175ºC, is due to the removal of six water coordinate molecules from the metallic center [13]. The second stage, between 180 and 420°C, is attributed to the ligand pyrolysis: a – initially involving two overlapped stages namely decarboxylation (in one or more stages) and b – the breakdown of the ethylenediamine structure with the formation of a stable intermediary compound (stable in temperature ranging from 420 up to 510°C). The last stage in this process, between 510 and 550°C, is due to the decomposition of stable intermediary compound with formation of magnesium oxide as residue.

*Calcium complex*

The TG and DTG curves, Fig. 2b and Table 3 show mass losses in five steps between 200 and 750ºC, as suggested from the DTG curve. The first stage from 200 to 630ºC begins with two overlapped events ascribed to the: a – elimination of two water molecules coordinated to the calcium ion and subsequent ligand pyrolysis with the ligand decarboxylation (in one or two stages) and b – breakdown of the ethylenediamine structure with calcium carbonate formation. The last stage, between 630 and 750ºC, is due to the thermal decomposition of the carbonate with the formation of calcium oxide as residual compound.

*Strontium complex*

The TG and DTG curves, Fig. 2c and Table 3 show mass losses in four steps, between 40 and 460ºC. The first stage from 40 up to 210ºC is attributed to the loss of two hydration water ($2H_2O$). The second stage, between 210 and 460ºC is ascribed to ligand pyrolysis: a – starting with the ligand decarboxylation and b – breakdown of the ethylenediamine structure with strontium carbonate formation as final residue, stable up to 820°C. The last stage, which starts at 850°C, is ascribed to the thermal decomposition of the strontium carbonate.

*Barium complex*

The TG and DTG curves, Fig. 2d and Table 3 show mass losses in four steps, between 40 and 480ºC. The first stage, up to 190ºC, is due to the dehydration with loss of $1.5H_2O$. The second stage, between 200 and 480ºC, is attributed to: a – a simultaneous loss of one strong coordinated water molecule and ligand pyrolysis, as

observed to calcium complex, with subsequent barium carbonate formation at 470°C. The final residue is stable up to 900°C.

**Table 3** Temperature range and the percentage of mass loss observed in each step of the TG curves of the complexes $[M(H_2O)_m(H_2Y)]\cdot nH_2O$

| Compound | | Steps | | | | |
|---|---|---|---|---|---|---|
| | | first | second | third | fourth | fifth |
| $[Mg(OH_2)_6(H_2Y)]$ | $\Delta T$/°C | 90–175 | 190–330 | 330–420 | 420–550 | – |
| | Mass loss/% | 25.65 | 21.33 | 19.77 | 23.56 | – |
| $[Ca(OH_2)_2(H_2Y)]$ | $\Delta T$/°C | 200–270 | 270–375 | 375–450 | 450–535 | 630–750 |
| | Mass loss/% | 22.27 | 19.62 | 15.40 | 15.51 | 11.98 |
| $[Sr(H_2Y)]\cdot 2H_2O$ | $\Delta T$/°C | 40–220 | 210–370 | 370–405 | 405–460 | 850 |
| | Mass loss/% | 13.20 | 20.81 | 16.84 | 13.60 | – |
| $[Ba(OH_2)_6(H_2Y)]\cdot 1.5H_2O$ | $\Delta T$/°C | 40–190 | 200–355 | 355–405 | 405–470 | – |
| | Mass loss/% | 5.64 | 19.94 | 20.81 | 11.92 | – |

$H_2Y$=Dihydrogenethylenediaminetetraacetate anion ($H_2Y^{2-}$)

The DSC curves of the synthesized complexes are shown in Fig. 3. All the thermal events observed in these curves are in agreement with the mass losses of the TG curves.

For the magnesium complex, Fig. 3a the endothermic peak at 195ºC is ascribed to the elimination of six water molecules coordinated to the magnesium ion, and this result is in agreement with the literature data [13]. The exothermic signals set, between 250 and above 600ºC, indicating three overlapping thermal events, are attributed to the thermal decomposition of the complex with formation of magnesium oxide.

In the calcium complex, Fig. 3b, the endothermic peak at 265ºC is attributed to the loss of coordinated water and subsequent ligand decomposition. The exothermic signals set between 290 and 600ºC, with evidence of three events, are attributed to the thermal decomposition of the complex with formation of calcium carbonate.

For the strontium complex, Fig. 3c, the endothermic peaks at 70 and 115ºC, are attributed to the elimination of hydration water. There is an endothermic peak at 265ºC and a broad exothermic one between 380 and above 600ºC, which are due to the thermal decomposition of the anhydrous complex with formation of strontium carbonate.

For the barium complex, Fig. 3d, the endothermic peaks at 105 and 250°C are attributed to the loss of hydration and strongly coordinated water, respectively. However, as observed for the calcium complex, the ligand only starts to decompose after the removal of coordinated water molecules from the metallic center. Figures 3b and d show a great similarity in the DSC curve profile of barium and calcium complex. This similarity gives support to believe that the water molecules are found

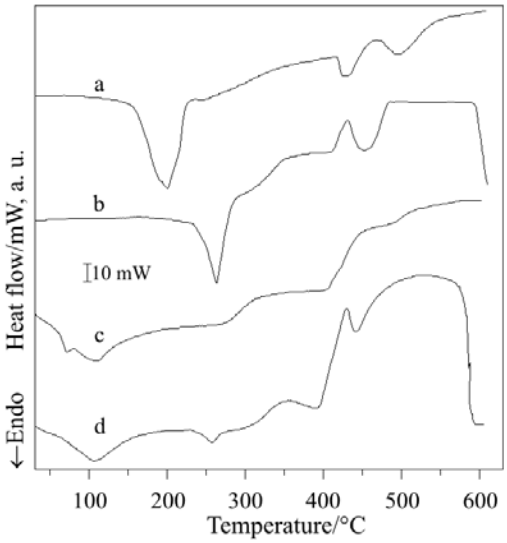


**Fig. 3** DSC curves of the complexes: a – $[Mg(OH_2)_6(H_2Y)]$, b – $[Ca(OH_2)_2(H_2Y)]$, c – $[Sr(H_2Y)]\cdot 2H_2O$, d – $[Ba(OH_2)(H_2Y)]\cdot 1.5H_2O$. $30 \leq \Delta T \leq 900$°C, $\beta$=20°C min$^{-1}$, air flow=150 mL min$^{-1}$, perforated aluminium 1 mm crucible

strongly coordinated to the metallic center, as suggested previously to the calcium complex.

The exothermic signals set between 300 and 580ºC, with evidence of peaks at 345, 420 and 520ºC, is ascribed to the thermal decomposition of the complex with the formation of barium carbonate.

## Conclusions

The X-ray powder diffraction patterns reveal that the magnesium and calcium complexes have a crystalline structure and that the strontium and barium complexes present an amorphous state.

The results of the present work have provided information about the thermal behaviour of the alkali earth metals (except beryllium and radium) chelates of dihydrogenethylenediaminetetraacetate anion. The result for the calcium complex is in agreement with those already described in literature, but not with that described for the barium complex.

For the magnesium and strontium complexes, their thermal behaviour has been reported for the first time.

* * *

The authors are grateful to FAPESP and CNPq for financial support.

## References


1 T. Moeller, F. A. J. Moss and R. H. J. Marshall, Am. Chem. Soc., 77 (1955) 3182.
2 T. Sawyer and P. J. Paulsen, J. Am. Chem. Soc., 81 (1959) 816.
3 M. L. Morris, R. W. Dunham and W. W. Wendlandt, J. Inorg. Nucl. Chem., 20 (1961) 274.
4 W. W. Wendlandt, Anal. Chem., 32 (1960) 848.
5 W. W. Wendlandt and G. R. Horton, Nature, 187 (1960) 769.
6 R. S. Kolat and J. E. Powell, Inorg. Chem., 1 (1962) 485.
7 R. G. Charles, J. Inorg. Nucl. Chem., 28 (1966) 407.
8 T. R. Bhat and R. Iyer Krishna, J. Inorg. Nucl. Chem., 29 (1967) 179.
9 A. Mercadante, M. Ionashiro, L. C. S de Oliveira, C. A. Ribeiro, D'Assunção and L. Moscardini, Thermochim. Acta, 216 (1993) 267.
10 M. S. Crespi, C. A. Ribeiro and M. Ionashiro, Thermochim. Acta, 221 (1993) 63.
11 T. Rojo, M. Insausti, M. I. Arriortua, E. Ernandez and J. Zubillaga, Thermochim. Acta, 195 (1992) 95.
12 M. Insausti, J. L. Pizarro, L. Lezama, R. Cortes, E. H. Bocanegra, M. I. Arriortua and T. Rojo, Chemistry of Materials, 6 (1994) 707.
13 M. O'Donnell Julian, V. W. Day and J. L. Hoard, Inorg. Chem., 12 (1973) 1754.
14 L. A. Zasurskaya, V. B. Rybakov, A. L. Posnyak and T. N. Polynova, Russ. J. Coord. Chem., 26 (2000) 492.
15 L. A. Zasurskaya, I. N. Polyakova, A. L. Posnyak, T. N. Polynova and V. S. Sergienko, Crystallography reports, 46 (2001) 377.
16 A. S. Antsyshkina, G. G. Sadikov, A. L. Posnyak and V. S. Sergienko, Russ. J. Coord. Chem., 47 (2002) 39.
17 Complex des Programme, CNRS, France 1990.
18 E. Milaré, F. L. Fertonani, M. Ionashiro and A. V. Benedetti, J. Therm. Anal. Cal., 59 (2000) 617.
19 E. Y. Ionashiro and F. L. Fertonani, Thermochim. Acta, 383 (2000) 153.